Free ammonia inhibition in microalgae and cyanobacteria grown in wastewaters: photo-respirometric evaluation and modelling

Simone Rossi[1], Rubén Díez-Montero[2], Estel Rueda[3], Federico Castillo Cascino[4], Katia Parati[4], Joan García[2], Elena Ficara[1,*]

[1] Politecnico di Milano, Department of Civil and Environmental Engineering (DICA), P.zza L. da Vinci, 3, 20133 Milan, Italy

[2] GEMMA-Group of Environmental Engineering and Microbiology, Department of Civil and Environmental Engineering, Universitat Politècnica de Catalunya-BarcelonaTech, c/ Jordi Girona 1-3, Building D1, 08034 Barcelona, Spain

[3] GEMMA-Group of Environmental Engineering and Microbiology, Department of Civil and Environmental Engineering, Escola d'Enginyeria de Barcelona Est (EEBE), Universitat Politècnica de Catalunya-BarcelonaTech, Av. Eduard Maristany 16, Building C5.1, 08019 Barcelona, Spain

[4] Istituto Sperimentale Italiano Lazzaro Spallanzani, Località La Quercia, 26027 Rivolta d'Adda, Italy

[*] Corresponding author (elena.ficara@polimi.it)

Abstract: The inhibitory effects of free ammonia (FA) on microalgae/cyanobacteria in wastewater-treating photobioreactors (PBR) can strongly reduce their treatment efficiency, increasing the operational costs and undermining the stability of the system. Although FA-promoting conditions (high pH, temperature and ammoniacal nitrogen concentration) are commonly met in outdoor PBRs, photosynthesis inhibition from FA has been scarcely explored and is rarely considered in microalgae-bacteria growth models. Two pilot systems and a series of lab-scale monocultures were tested using a photo-respirometry approach, to evaluate the effects of FA (8.5 - 136 mg NH_3 L^{-1}) on photosynthesis. Two mathematical inhibition models were compared, with the aim of selecting best-fitting equations to describe photo-respirometric experiments. A set of calibrated inhibition parameters was obtained for microalgae and cyanobacteria, growing in monocultures or in mixed algae-bacteria consortia. Cyanobacteria

were more sensitive to FA than green microalgae and mixed phototrophs-bacteria consortia showed a higher resistance compared to monocultures. Estimated inhibition parameters were used to describe common operational/environmental conditions in algae-bacteria systems, demonstrating the potential drop in photosynthetic activity under those relevant operational conditions.

Keywords: Free ammonia inhibition; Photosynthetic oxygenation modelling; Wastewater treatment; Microalgae and cyanobacteria; Algae/bacteria consortia

Highlights:

- Free ammonia inhibition was studied in *chlorophyceae* and cyanobacteria
- Both monocultures and mixed phototrophs-bacteria consortia were investigated
- The EC_{50} for free ammonia was higher for green microalgae than cyanobacteria
- The EC_{50} was higher in mixed phototrophs-bacteria consortia than in monocultures
- Free ammonia inhibition is modelled under common weather/operational conditions

1. INTRODUCTION

The design and operation of conventional biological wastewater treatment processes, such as activated sludge or anaerobic processes, rely on exhaustive knowledge, standardized methodologies and robust mathematical modelling, allowing to achieve high and stable removal efficiencies (van Loosdrecht et al., 2016). Aerobic processes are especially characterized by severe limitations: i) high operational costs and energy requirements for the aeration of mixed liquor and sludge dewatering (Plappally & Lienhard, 2012) and ii) high environmental

impacts for direct and indirect greenhouse gases (CO_2, CH_4 and N_2O) emissions (Campos et al., 2016). In the last years there has been a renewed interest in microalgae treatment systems, because it has been shown that growing microalgae/cyanobacteria in consortia with wastewater-associated bacteria, can lead to significant advantages, while guaranteeing effluent quality (Muñoz et al., 2006; Campos et al., 2016). In fact, the algae-bacteria metabolites exchange (CO_2 and O_2), can significantly reduce costs for aeration. Moreover, sludge disposal costs can be reduced by recovering nutrients (biofertilizers/biostimulants) and/or energy (biogas) from the algal-bacterial biomass (Moreno-García et al., 2017). Phototrophic microorganisms can adapt and survive in extreme environmental conditions but some compounds, such as antibiotics, herbicides/pesticides, heavy metals or unionized NH_3 (or free ammonia, FA), can cause a severe inhibition of photosynthesis, hampering the biological activity and therefore reducing the oxygen supply by phototrophs and mining the efficiency of the system.

FA has been identified as an important short-term and species-specific inhibitor of the photosynthetic process, with some species being particularly resistant to elevated concentrations of ammonia and other being much more sensitive (Collos & Harrison, 2014; Markou et al., 2016; Gutierrez et al., 2016). The inhibition of photosynthesis can be associated to different mechanisms of action: i) ammonia causes damages to the oxygen evolving complex (OEC) of the photosystem II, acting as an uncoupler of the Mn cluster of the OEC and displacing a water ligand (Drath et al., 2008; Markou and Muylaert, 2016; Markou et al., 2016); ii) ammonia diffuses through membranes and

accumulates, acting as an uncoupler and disrupting the ΔpH component of the thylakoid proton gradient (Belkin and Bossiba, 1991, Markou and Muylaert, 2016; Gutierrez et al., 2016). Besides these effects, the activity of photosystem I and the dark respiration rates are also negatively affected by FA and ammonia toxicity also seems to be amplified at elevated light intensities, although the mechanisms are not fully understood (Markou et al, 2016). Quantifying the inhibition of photosynthetic activities is of particular interest in algae-based wastewater treatment processes (Abeliovich & Azov, 1976; Kallqvist and Svenson, 2003; Tan et al., 2016; Goto et al., 2019). Indeed**,** the equilibrium reaction between FA and ammoniacal nitrogen (NH_4^+) shifts toward FA under the following conditions: i) high pH values associated to photosynthetic processes, ii) high temperatures due to atmospheric conditions and iii) high total ammoniacal nitrogen (TAN = NH_3 + NH_4^+) concentrations (Anthonisen et al., 1976; Collos and Harrison, 2014). The inhibition of photosynthesis due to the presence of FA could be assessed in different ways: by carrying out batch growth experiments (Källqvist and Svenson, 2003; Gutierrez et al., 2016; Bo et al., 2016; Zhao et al., 2019); by measuring the uptake of nutrients or oxygen (Abeliovich and Azov , 1976; Azov and Goldman, 1981; Boussiba et al., 1991; Dai et al., 2008; Segura et al., 2017), or by coupling pulse-amplitude modulation (PAM) with photo-respirometry or with some of the aforementioned techniques (Drath et al., 2008; Markou et al., 2016; Markou and Muylaert, 2016; Li et al., 2019; Wang et al., 2019). Despite the relevance of FA inhibition, and the availability of mathematical models to describe this phenomenon (e.g., Andrews, 1968; Han and Levenspiel, 1987, among others), FA inhibition is

rarely considered when analysing and modelling the evolution of microalgae-bacteria consortia (Shoener et al., 2019). In addition, FA inhibition assays on microalgae-bacteria suspensions are not documented in literature, and almost all experimental works are performed on axenic cultures using synthetic media, apart from a few cases (Hernandèz et al., 2013; Beyl et al., 2019).

The objectives of this study were to quantify the inhibition of photosynthesis due to FA in different phototrophic organisms, and to identify a mathematical photo-oxygenation model, describing FA inhibition under typical operational conditions in microalgae/cyanobacteria-based bioremediation systems. Photo-respirometric tests (PRT) were carried out on cyanobacteria and green microalgae monocultures and on mixed phototrophs-bacteria suspensions dominated by microalgae and cyanobacteria, in order to analyse the inhibition of different phototrophic microorganisms exploited in wastewater treatment. In view of standardizing PRTs and comparing the results obtained with other literature works, a detailed description of experimental procedures was also included and discussed. The obtained dataset was used to compare two different models (a simple non-competitive inhibition model and a logistic sigmoidal function), and best-fit equations were used to describe common operational/environmental conditions in algae-bacteria systems, demonstrating the significance of the potential drop in photosynthetic oxygenation due to the presence of FA. To the best knowledge of authors, this is the first study in which the effects of FA on the photosynthetic activity of eukaryotic microalgae and cyanobacteria were directly compared, using data from both monocultures and mixed algae-bacteria consortia.

2. MATERIALS AND METHODS

2.1. Microorganisms and cultivation systems

2.1.1. Pilot-scale phototrophs-bacteria cultivation systems

Microalgae-bacteria

The microalgae-bacteria consortium was grown in a pilot-scale high rate algal pond (HRAP) (volume: 1.2 m^3, surface = 5.8 m^2, liquid height = 0.2 m) located at the Bresso-Niguarda wastewater treatment plant (WWTP) (Milan, Italy). The liquid fraction of anaerobically digested sludge (LFAD) was separated by centrifugation and used to feed the HRAP, having demonstrated good characteristics as growth substrate. More information about the wastewater characterisation is reported in previous studies (Mantovani et al., 2019; Marazzi et al., 2019). The pilot scale HRAP was installed outdoor and covered with a polycarbonate roof to protect the pond from rain. The HRAP was inoculated with the microalgae-bacteria suspension with *Chlorella sp*. and *Scenedesmus sp*. as the dominant species and operated in continuous with undiluted LFAD as the feed at an average hydraulic retention time (HRT) of 10 d for seven months (April 2019 - October 2019).

Cyanobacteria-bacteria

The cyanobacteria-bacteria consortia were grown in a set of three demonstrative-scale tubular semi-closed photobioreactors (PBR) (volume = 11.7 m^3 each), located in the Agròpolis experimental campus of Universitat

Politècnica de Catalunya (UPC) (Barcelona, Spain). Detailed information about PBRs design, start-up and operations characterisation is available in García et al. (2018). In brief, each PBR consisted of 2 lateral open tanks connected through 16 transparent tubes (diameter = 125 mm, length = 47 m). Each tank was equipped with a paddle wheel ensuring proper mixing and circulation of the suspension through the tubes and the reduction of excess dissolved oxygen (DO). The three PBRs were connected in series to promote the selection of cyanobacteria and the production and the accumulation of biopolymers, using agricultural runoff as feedstock medium. Nutrient concentrations in the first PBR were adapted to reach the optimum ratio favouring the growth of cyanobacteria over green microalgae, by adding an external source of NO_3 (potassium nitrate inorganic fertilizer, NK13-46, 13% N-NO_3). The culture was mainly dominated by cyanobacteria of the species *Synechococcus* sp. and *Synechocystis* sp. In the second PBR, a feast and famine regime was applied by adding an external inorganic carbon source during 6 h d^{-1}, in order to enhance the cyanobacterial carbon uptake efficiency and subsequent biopolymers accumulation. In the third PBR, the inorganic carbon was continuously provided to increase the accumulation of biopolymers after the feast and famine phase. CO_2 and sodium bicarbonate ($NaHCO_3$) were used as external inorganic carbon source in both the second and third PBRs. CO_2 was injected by means of diffusers in the lateral open tanks of the PBRs and regulated by a pH-control system. $NaHCO_3$ was added by a daily dose of a concentrated solution of $NaHCO_3$. Detailed information about the operational strategies adopted, wastewater characteristics

and biopolymers production can be found elsewhere (Díez-Montero et al., 2019, Rueda et al., submitted).

2.1.2. Cultivation of green microalgae and cyanobacteria monocultures

Green microalgae

Four different species of green microalgae were selected after microscope observations in the HRAP and cultured in the laboratories of the *Istituto Sperimentale Italiano Lazzaro Spallanzani* (Rivolta d'Adda, IT). In particular, two strains of *Chlorella spp.* (*Chlorella vulgaris, SAG211-11j and Chlorella sorokiniana, SAG211-8k*) and one strain of *Scenedesmus* (*Scenedesmus quadricauda, or Desmodesmus armatus, SAG276-4d*) were acquired from the Culture Collection of Algae at the University of Göttingen (SAG, Germany), while one strain of *Scenedesmus spp.* (identified as *Scenedesmus obliquus*) was isolated from an outdoor pond. All strains were cultured in 500 mL glass Erlenmeyer flasks, using commercially available Modified Bold Basal Medium (MBBM, Sigma-Aldrich), at room temperature (20 - 25 °C) and under controlled irradiance (cool white fluorescent lamps, Philips F58W/33-640 58W) and 12 h/12 h light/dark (L/D) cycles. Sterile air (0.2 µm cutoff) was bubbled in the PBRs to provide carbon dioxide and mixing. The cultivation of green microalgae was achieved without pH-control.

Cyanobacteria

Three different species of cyanobacteria were identified and isolated from the semi-closed PBRs fed with agricultural runoff and cultured under controlled conditions: *Synechococcus* sp., *Synechocystis* sp., and *Leptolyngbya* sp. The strains were sampled from the first semi-closed PBR and inoculated in plates prepared with 1% bacteriological agar and commercially available BG11 medium (Sigma-Aldrich, St. Louis, US), by direct streaking or after serial dilutions in saline media, as explained in Rueda et al. (2020). Once cyanobacteria colonies were obtained, they were transferred into 2 mL of medium contained in 15 mL test tubes and scaled-up (scaling ratio = 1:5), until 1 L cultures were obtained. Finally, they were kept in Erlenmeyer flasks at room temperature (30 ± 2°C), under controlled irradiance (approximately 36.2 µE m^{-2} s^{-1} using 14W cool-white LED lights) under 15 h/9 h L/D cycles. Sterile air (0.2 µm cutoff) was bubbled to provide mixing and CO_2 and to remove accumulated DO. The cultivation was achieved without pH-control. More information about the cultivation of cyanobacteria monocultures can be found elsewhere Rueda et al. (2020).

2.2. Respirometric unit

The activity of phototrophic organisms was evaluated using a fully equipped photo-respirometric/titrimetric unit, provided with different options for DO- and pH-control. The photo-respirometer (IDEA Bioprocess Technologies s.r.l.) includes: a closed bioreactor (0.5 L glass bottle, DURAN protect, GLS80 headplate), a gas injection system (an airpump and a gas cylinder connected to

a set of electro-valves), a signal/communication and mixing (0 - 300 RPM) unit and an acid/base dosage system (two 0 - 12 RPM peristaltic pumps). The DO-control system was made of a DO probe (Hamilton VisiFerm, DO Arc 120) and a DO-stat system by O_2/N_2 bubbling, while the pH-control system was made of a pH probe (Hamilton Polylite Plus, H Arc 120) and a pH-control system by CO_2 bubbling or acid/base dosage. The entire system was controlled with an industrial grade PC running a LabView-based control software (Figure 1). The sampling interval for temperature, pH and DO data was set to 3 s. During cyanobacteria and cyanobacteria-bacteria tests, the light source was an incandescent light bulb (30 W), providing a photosynthetically active radiation (PAR) level of about 116 ± 23 µE m^{-2} s^{-1}. During microalgae and microalgae-bacteria tests, irradiance and temperature were controlled by placing the vessels into a thermostatic chamber provided with irradiance and air temperature regulation (F.lli Della Marca s.r.l., TS series). In this case, four internal fluorescent elements (OSRAM L36W/965 - Deluxe cool daylight) were switched on/off, reaching a similar light intensity as the one obtained for tests performed on cyanobacteria (108 ± 16 µE m^{-2} s^{-1}). The incident PAR radiation at 400 - 700 nm was measured along the internal surface of the glass bottle by using a quantum sensor (Apogee Instruments, MQ-500).

2.3. Experimental procedures, test conditions and set of experiments

The effects of FA concentrations were assessed under standardized condition with respect to: incident irradiance (110 µE m^{-2} s^{-1}), pH (8.5) and temperature

(20 °C). The DO concentration was maintained in the range 100 - 130% of the DO saturation at the test temperature by air bubbling. For cyanobacteria, FA was tested at 8.5, 17, 34 and 68 mg NH_3 L^{-1}, while microalgae were exposed to higher concentrations, i.e. 17, 34, 68 and 136 and mg NH_3 L^{-1}, due to the higher tolerance to ammonium/ammonia reported in literature (Collos & Harrison, 2014). The selected range of FA concentrations was typically used in previous FA inhibition assays, adequately covering the values expected during microalgae-/cyanobacteria-based bioremediation and including quite high FA concentrations to represent the case of high strength wastewaters with high TAN concentrations (e.g. anaerobic digestates, landfill leachates). A total of seven pure microalgae/cyanobacteria samples and four mixed microalgae-/cyanobacteria-bacteria consortia were used for activity assessments at different FA concentrations. A summary of performed PRTs and test conditions is reported in Table 1.

The test protocol was defined by slightly modifying a standardized protocol, adopted for calibrating microalgae-bacteria models and evaluating best equations to describe the effects of environmental conditions (Rossi et al., 2018; Rossi et al., 2020a; Rossi et al., 2020b). The protocol included the following steps: 1) sampling/transportation, 2) pre-treatments, 3) sample characterisation, 4) addition of nitrifying inhibitors (except for monocultures), 5) addition of nutrient solutions (except for monocultures), 6) acclimation to test conditions (1.5 h), 7) excess DO removal, 8) alternation of L/D phases with (inhibited reactor) and without (control reactor) NH_3 additions, 9) data processing/modelling. Some of these aspects are discussed below.

2.3.1. Pre-treatments

The samples were taken from the lab-scale cultivation systems and diluted with fresh media (MBBM and BG11 for microalgae and cyanobacteria monocultures, respectively), for reaching the desired optical density at 680 nm (OD_{680}) and ensuring nutrient availability. After preliminary evaluations of the volumetric oxygen production and uptake rates (OPR and OUR, respectively) at different light intensities (data not shown), the initial OD_{680} was set to 0.2 to conduct PRTs under optimal (i.e. non-limiting and non-inhibiting) conditions of light availability, while avoiding a too fast DO accumulation in the vessel. The microalgae-bacteria suspension sampled from the HRAP were first screened with a 300 µm mesh to remove detached biofilms and inert particles. The suspension was concentrated by centrifugation (5000 RPM, 10 min) and an appropriate amount of biomass was resuspended into a nutrient-free mineral medium up to OD_{680} = 0.2. The mineral medium used for resuspension was designed to mimic the LFAD (Rossi et al., 2018), according to the average concentrations of metals (Na, Mg, Ca, K, Al, Mn, Fe, Co, Ni, Cu and Zn) in the algae-bacteria suspension. Regarding cyanobacteria-bacteria consortia, the biomass developed in the semi-closed PBRs contained filamentous cyanobacteria flocs, making it difficult to determine the OD_{680}. Therefore, total suspended solids (TSS) concentrations were used to evaluate the amount of biomass to be diluted in the effluent of each PBR. Dilution with the effluent was preferred to dilution with synthetic media, since it was not possible to characterize the ionic composition of semi-closed PBRs suspensions.

2.3.2. Addition of bacterial inhibitors and nutrient solutions

During PRTs performed on mixed cultures of phototrophs/bacteria, Allylthiourea (ATU, 10 mg L^{-1}) was added to inhibit nitrifying activity while the photosynthetic activity remained unaffected (Rossi et al., 2018; Rada-Ariza, 2018). Inorganic nutrients were also supplied in a control reactor, to determine the maximum photosynthetic activity, by injecting concentrated solutions of NH_4Cl, K_2HPO_4 and $NaHCO_3$ (15 mg N-NH_4^+ L^{-1}, 5 mg P-PO_4^{3-} L^{-1}, 150 mg C-HCO_3^- L^{-1}). The background FA concentration corresponding to the NH_4Cl injection was approximately 1.7 mg NH_3 L^{-1}. The total volume of injected solutions (nutrients, inhibitors and acid/base titrants) did not substantially modify the biomass concentration and thus of the light extinction in the respirometer (maximum volume increase: 4%). Nutrients and bacterial inhibitors were not added during PRTs performed on microalgae/cyanobacteria monocultures, as the nutrient availability was guaranteed by the resuspension in the mineral medium.

2.3.3. Acclimation to test conditions and L/D phases

Before starting each PRT, the biomass was incubated under the test conditions (1.5 h), for an equilibration of metabolic activities to the new light, temperature and pH. During PRTs, the biomass was exposed to light for 10 min, and then kept in the dark for 20 min. In the control reactor, this L/D cycle was repeated from three to six times for improving statistical significance and identifying stable initial conditions in terms of volumetric OPRs and OURs. In the inhibited

reactor, concentrated ammonia solutions were dosed at the beginning of each light phase.

2.4. Data processing and calculations

2.4.1. Calculation of oxygen production rates

The DO dynamics was modelled by considering the concomitant occurrence of (i) either a constant net photosynthetic oxygen production rate (during L phases) or a respiratory oxygen uptake rate (during D phases), and (ii) the oxygen mass transfer rate at the liquid-gas interface (OTR). The resulting dynamic mass balance for the DO in the photo-respirometer is therefore (Equations 1-3):

$$\begin{cases} \frac{d(DO)}{dt} = OPR_{NET,i} + OTR & \text{(Light phases, } L_i \text{ i=1, …, 5)} \\ \frac{d(DO)}{dt} = OUR_{RESP,i} + OTR & \text{(Dark phases, } D_i \text{ i=1, …, 5)} \end{cases} \#(1)$$

$$OTR = \theta^{(T-293.15)} * k_L a_{20} * (DO_{SAT} - DO) \#(2)$$

$$DO_{SAT} = pO_2 * K_{H,O_2}(T) = pO_2 * K_{H,O_2,\ REF} * \exp\left(-\frac{-\Delta_{SOL}H}{R} * \left(\frac{1}{T} - \frac{1}{T_{REF}}\right)\right) \#(3)$$

Where: DO [mg O_2 L^{-1}] is the DO concentration at the time t [h], OPR_{NET},i [mg O_2 L^{-1} h^{-1}] is the average net OPR during the ith light phases L_i, OUR_{RESP},i [mg O_2 L^{-1} h^{-1}] is the average respiratory OUR during the ith dark phases D_i, OTR is the oxygen mass transfer rate [mg O_2 L^{-1} h^{-1}], DO_{SAT} [mg O_2 L^{-1}] is the DO saturation concentration at the temperature T [K], pO_2 = 0.21 [Atm] is the partial pressure of oxygen in atmosphere, T_{REF} = 298.15 [K] is the reference temperature, $K_{H,O2}(T)$ [mg O_2 L^{-1} Atm^{-3}] is the value of Henry's law solubility constant for oxygen at the temperature T, $K_{H,O2,REF}$ = 40.5 [mg O_2 L^{-1} Atm^{-1}] is

the value of Henry's law solubility constant at T_{REF} (Sander, 2015), k_La_{20} = 0.17 ± 0.07 [h^{-1}] is the volumetric oxygen mass-transfer coefficient evaluated at 20 °C during abiotic tests, that was previously assessed for the photo-respirometer, according to the nonlinear regression method (ASCE, 1993).

To compute the average $OPR_{NET,i}$ and $OUR_{RESP,i}$ and k_La, nonlinear least square regression was performed using the *lsqcurvefit* function with the software MATLAB R2019b (Optimisation Toolbox™, The MathWorks, Inc., USA). Raw DO data were fitted to estimate OPR_{NET} and OUR_{RESP}. According to the methodology adopted in previous studies (Choi et al., 2010; Tang et al., 2014; Najnm et al., 2017; Rossi et al., 2018), the gross OPR (OPR_{GROSS}) was then calculated for each L_i/D_i determination, by subtracting the estimated OUR_{RESP} to the OPR_{NET}, and the result was divided by the TSS of the sample, measured according to Standard Methods (APHA, 2017), to obtain specific OPRs and OURs ($sOPR_{GROSS}$ and $sOUR_{RESP}$, [mg O_2 g TSS^{-1} h^{-1}]) (Equations 5-7):

$$OPR_{GROSS,i}=OPR_{NET,i}-OUR_{RESP,i} \text{ (Phases 1, 2, 3)} \quad \#(4)$$

$$sOPR_{GROSS,i}=\frac{OPR_{GROSS,i}}{TSS} \text{ (Light phases, } L_i \text{ i=1, 2, 3)} \quad \#(5)$$

$$sOUR_{RESP,i}=\frac{OUR_{RESP,i}}{TSS} \text{ (Dark phases, } D_i \text{ i=1, 2, 3)} \quad \#(6)$$

All models were fitted against $sOPR_{GROSS}$.

2.4.2. Inhibition models definition and selection

The concentration of FA was calculated as a function of temperature, pH and of total ammoniacal nitrogen (TAN) concentration (Anthonisen et al., 1976) (Equation 7):

$$NH_3 = TAN * \frac{MW_{NH_3}}{AW_N} * \frac{10^{pH}}{\exp\left(\frac{6344}{T}\right) + 10^{pH}} \quad \#(7)$$

Where: TAN = $NH_3 + NH_4^+$ [mg N L^{-1}] is the total ammoniacal nitrogen, MW_{NH3}, is the molecular weight of ammonia [g NH_3 mol NH_3^{-1}], AW_N is the atomic weight of nitrogen [g N mol N^{-1}], pH is the pH of the suspension [-], T is the temperature of the suspension [K].

Two different inhibition models were chosen to describe the effect of FA on the photosynthesis and respiration: the non-competitive inhibition model (Equation 8) used to evaluate FA inhibition in anaerobic digestion models (Angelidaki et al., 1993) and a sigmoidal logistic curve, or Hill-type model (Equation 9), used to describe dose-response curves (Prinz et al., 2010).

$$f_{NH_3} = \frac{sOPR_{NH3}}{sOPR_{CONTROL}} = \frac{1}{1 + \frac{NH_3}{EC_{50,NH3}}} \quad \#(8)$$

$$f_{NH_3} = \frac{sOPR_{NH3}}{sOPR_{CONTROL}} = 1 - \frac{1}{1 + \left(\frac{EC_{50,NH3}}{NH_3}\right)^N} \quad \#(9)$$

Where: $sOPR_{NH3}$ is the gross sOPR calculated in the reactor subject to FA inhibition [mg O_2 g TSS^{-1} h^{-1}], $sOPR_{CONTROL}$ is the gross sOPR calculated in the control reactor [mg O_2 g TSS^{-1} h^{-1}], NH_3 is the calculated initial FA concentration [mg NH_3 L^{-1}], $EC_{50,NH3}$ is the inhibition parameter of the non-competitive inhibition model and the Hill model, representing the FA concentration causing a 50% inhibition of the photosynthetic activity [mg NH_3 L^{-1}], N is the dimensionless shape parameter of the Hill model [-].

The models were applied to the dataset and different information criteria were calculated, to select for the most appropriate model. In particular, the adjusted R-squared (R_{ADJ}^2, equation 10) was calculated to evaluate the goodness of fit, and the model resulting in a lower value of the Akaike Information Criterion corrected for small samples (cAIC, equation 11, Hurvich and Tsai, 1991), was considered as the most suitable to represent experimental results:

$$R_{ADJ}^2 = 1 - \left(\frac{n-1}{n-p}\right) * \frac{SSE}{SST} \quad \#(10)$$

$$cAIC = \frac{SSE}{n} * (1+2*p) + 2*p*\left(\frac{p+1}{n-p-1}\right) \quad \#(11)$$

Where: n is the number of experimental observations, p is the number of model parameters, SSE is the sum of squared error and SST is the sum of squared difference between each datum and the mean value of all data.

2.4.3. **Statistical analysis**

An unbalanced one-way analysis of variance (ANOVA) was applied to the datasets of experiments performed on microalgae and cyanobacteria, to evaluate statistically significant differences (α = 0.05) between calculated values of inhibition parameters for monocultures and mixed groups. The software MATLAB R2019b was used for the analysis (Statistics and Machine Learning Toolbox™, function *anova1*).

2.5. **Definition of free ammonia inhibition scenarios under typical operational conditions**

To evaluate the need for considering FA inhibition in algae/bacteria modelling, several scenarios were analysed by calculating theoretical FA concentration profiles during typical operational days in the pilot plants. Scenarios were defined by varying: i) the season (spring, summer and autumn), ii) the setpoint of the pH-control system (7, 8 and 9 for microalgae and 8.5, 9.5 and 10.5 for cyanobacteria) and iii) the initial TAN concentration in the suspension (5, 10 and 20 mg N-TAN L^{-1} for cyanobacteria and 35, 70 and 140 mg N-TAN L^{-1} for microalgae). Typical daily patterns were defined for incident PAR and water temperature by averaging hourly data collected over a long-term period (January 2017 - November 2019) (Figure 3). Irradiance data were collected from the closest weather stations located near each pilot-plant site, and water temperature was logged by temperature probes in pilot reactors. Daily average trends for each season are shown in Figure 3. The pH setpoints and TAN concentrations were chosen according to values measured in pilot plants during the photo-respirometric campaigns, in order to reflect relevant conditions that are commonly met in wastewater-treating outdoor PBRs. The measured pH value in the microalgae-bacteria system was on average 7.0 (maximum pH: 8.5), as a consequence of the high nitrification rates reported (Mantovani et al., 2019) and compared with the higher values measured in the cyanobacteria-bacteria systems (average pH = 8.4, maximum pH = 9.5). Likewise, the measured TAN concentration in the microalgae-bacteria system was on average = 34 mg N-TAN L^{-1} (maximum TAN = 71 mg N-TAN L^{-1}). This condition reflects the high concentration of NH_4^+ in the LFAD (240 ± 55 mg N-NH_4^+ L^{-1}, on average) and the presence of residual NH_4^+ concentration in the suspension,

possibly due to low transitory algal activities. On the contrary, cyanobacteria scenarios were characterized by lower TAN concentrations, as the influent was a low strength wastewater stream (agricultural runoff). The biomass was subject to starvation to promote the accumulation of biopolymers and fed with nitrate as nitrogen source, with the ammoniacal nitrogen being almost absent during the entire experimentation (average TAN = 0.3 mg N-TAN L^{-1}, maximum TAN = 2.9 mg N-TAN L^{-1}).

In addition to modelling FA inhibition, switch functions for light (f_I, Equation 12, Bernard and Rémond, 2012), temperature (f_T, Equation 13, Bernard and Rémond, 2012) and pH dependence (f_{pH}, Equation 14, Ippoliti et al., 2016) were evaluated to describe a more realistic photosynthetic sOPR trend, during typical days. The model describing the overall trend of oxygen production, f_{TOT} (equation 15), is the product of all the switch functions (Equation 8, and 12 - 14). f_{pH} is constant, as an ideal pH-control is implemented. No light/solute-gradients were included (0-D model), therefore average irradiance and perfect mixing are considered.

$$f_I = sOPR_{MAX} * \frac{I}{I + \frac{sOPR_{MAX}}{\alpha} * \left(\frac{I}{I_{OPT}} - 1\right)^2} \quad \#(12)$$

$$f_T = \frac{(T-T_{MAX})*(T-T_{MIN})^2}{(T_{OPT}-T_{MIN})*((T_{OPT}-T_{MIN})*(T-T_{OPT})-(T_{OPT}-T_{MAX})*(T_{OPT}+T_{MIN}-2*T))} \quad \#(13)$$

$$f_{pH} = \frac{(pH-pH_{MAX})*(pH-pH_{MIN})}{(pH_{OPT}-pH_{MIN})*((pH_{OPT}-pH_{MIN})*(pH-pH_{OPT})-(pH_{OPT}-pH_{MAX})*(pH_{OPT}+pH_{MIN}-2*pH))} \quad \#(14)$$

$$f_{TOT} = f_I * f_T * f_{pH} * f_{NH_3} \quad \#(15)$$

Where: $sOPR_{MAX}$ is the maximum sOPR obtained at the optimal light intensity [mg O_2 g TSS^{-1} h^{-1}], I is the actual irradiance [µE m^{-2} s^{-1}], α = 0.45 is a dimensionless shape parameter [-], I_{OPT} = 313 [µE m^{-2} s^{-1}] is the optimal light

intensity corresponding to the maximum photosynthetic activity, T is the actual temperature of the suspension [°C], T_{MAX} = 41.7 [°C] is the maximum temperature above which the photosynthetic activity stops, T_{OPT} = 28.1 [°C] is the optimal temperature corresponding to the maximum photosynthetic activity, T_{MIN} = 0.1 [°C] is the minimum temperature below which the activity stops, pH is the actual pH value [-], pH_{MAX} = 11.1 [-] is the maximum pH above which the activity stops, pH_{OPT} = 7.5 [-] is the optimal pH corresponding to the maximum photosynthetic activity, pH_{MIN} = 0.2 [-] is the minimum pH below which the activity stops.

The parameters characterizing the described switch functions were calibrated on the microalgae-bacteria consortium during a previous PRT campaign, in which the effects of a wide range of irradiance, temperature and pH values were assessed (Rossi et al., submitted). Since no experimental data were available to describe the effects of environmental conditions on cyanobacteria, and the optimal conditions for cyanobacteria can significantly differ from microalgal optima (Giannuzzi et al., 2019)**,** the evolution of switch functions was only modelled for the HRAP case study.

3. RESULTS AND DISCUSSION

3.1. Model selection

The experimental $sOPR_{GROSS}$ values were calculated as described in section 2.4 and the dataset obtained from PRTs was used to fit to the non-competitive inhibition model (equation 9) and to the sigmoidal logistic curve (equation 10).

Model information criteria (R_{ADJ}^2 and cAIC) are shown in Table 2. Both models can describe the entire photo-respirometric dataset and show a high value of R_{ADJ}^2 (all higher than 0.98). Regarding cAICs values, low differences among models are observed, however the non-competitive model was preferred because a similar predicting ability was obtained with one parameter less, thus reducing computational costs and facilitating parameter estimation. The predicting ability of this model was able to correctly describe the inhibition process for both mono and mixed cultures. However, the variability of some estimated parameter was quite high, as proven by the large extension of 95% confidence bounds. Predictions for cyanobacterial monocultures were more accurate than for microalgae. The highest variabilities were found for *Scenedesmus quadricauda* and *Chlorella sorokiniana.* With respect to this variability, decreasing the measurement noise (e.g. by reducing/eliminating gas-liquid transfer) and/or adjusting the experimental protocol (e.g. by increasing the number of replications to obtain more robust inhibition data) could be desirable improvements to the proposed methodology. Moreover, the variability of estimated parameters was generally higher in PRTs performed on mixed consortia, compared to monocultures (especially for the sample from the microalgae-bacteria system). This variability can be due to the presence of other microorganisms in the suspension, possibly contributing to the DO mass balance (protozoa, heterotrophic bacteria) and constituting an additional biological noise. In order to improve data reliability, further research is suggested regarding the pre-treatment of the sample and the possibility of using

wide spectrum inhibitors/antibiotics to suppress undesired in biological activities.

3.2. Effects of free ammonia on pure microalgae and mixed microalgae-bacteria consortia

Microalgae and cyanobacteria monocultures

Experimental $sOPR_{NH3}/sOPR_{CONTROL}$ values quantifying the reduction of photosynthetic activity due to the exposure to FA for microalgae and cyanobacteria monocultures are shown in Figure 2A and Figure 2B, respectively, together with the fit of the non-competitive inhibition model. The photosynthetic activities of all monocultures decreased at increasing FA, as expected due to the inhibitory effects on photosynthesis, and no stimulatory effects due to ammonia assimilation were observed. FA only affected the $sOPR_{NET}$, and the observed $sOUR_{RESP}$ did not vary significantly regardless of the FA concentration applied (data not shown), coherently with the findings of Abeliovich & Azov (1976). However, this behaviour might be species-specific and should not be generalized. For instance, Markou et al. (2016) measured decreasing respiration rates at increasing FA in *Arthrospira platensis sp.* and *Chlorella vulgaris sp.*

Regarding results on microalgae monocultures (Table 2), the value of $EC_{50,NH3}$ for *Chlorella vulgaris* (60.9 mg NH_3 L^{-1}) was close to 54 mg NH_3 L^{-1} obtained by Markou et al. (2016) under similar conditions. An $EC_{50,NH3}$ = 96.3 mg NH_3 L^{-1} was obtained for *Chlorella Sorokiniana*, coherently with the absence of inhibition reported by Gutierrez et al. (2016), and with the higher concentrations obtained

for different *Chlorella Sorokiniana* strains by Wang et al. (2019). The inhibition parameter for *Scenedesmus quadricauda* was 77.7 mg NH_3 L^{-1}, but literature values are not available for this species and a direct comparison is not possible. The value obtained for *Scenedesmus obliquus* (52.6 mg NH_3 L^{-1}) is instead very similar to that obtained at the same pH by Abeliovich & Azov (1976) (51 mg NH_3 L^{-1}). $EC_{50,NH3}$ for *Scenedesmus obliquus* (60.9 mg NH_3 L^{-1}) are slightly lower, but in the same order of magnitude, than what reported by Azov & Goldman (1982) and Collos & Harrison (2014).

Regarding cyanobacterial monocultures, estimated inhibition parameters and model fits are reported in Figure 2B. As mentioned, contrarily to other findings (Collos & Harrison, 2014), the adverse effect of FA on photosynthesis was more pronounced in cyanobacteria than in microalgae. This is confirmed by comparing the average $EC_{50,NH3}$ for the two types of organisms (Table 2). For cyanobacterial monocultures, the average $EC_{50,NH3}$ was 14.1 mg NH_3 L^{-1}, with similar values among the different strains adopted. Unluckily, only a few authors reported inhibition parameters for cyanobacteria, and most available data are for the strain *Arthrospira platensis sp.*, typically characterized by a high resistance to FA (Markou et al., 2014; 2016). However, all the values obtained for cyanobacterial monocultures and mixed populations fall in the range indicated by Collos & Harrison (2014) (4.3 - 34.8 mg NH_3 L^{-1}).

Mixed phototrophs-bacteria consortia

The value of $EC_{50,NH3}$ for the mixed microalgae-bacteria consortium was among the highest and also the coefficients determined for cyanobacteria mixed

cultures were higher than those obtained from monocultures data. Due to the increase in the $EC_{50,NH3}$ for both microalgae and cyanobacteria monocultures to mixed cultures (Table 2), a first interpretation of results would suggest that the environmental conditions in which the mixed cultures are grown selected phototrophic strains that are more robust and tolerant to adverse conditions, including inhibitory compounds. Unravelling this aspect would contribute to a better understanding of the interactions between microorganisms in wastewater treatment processes with microalgae-bacteria (e.g., optimizing influent TAN loading rates, or adopting dynamic pH setpoints based on TAN).

However, the difference in the effect of FA on microalgae mixed and monocultures could not be explained by ANOVA (*p-value* = 0.501), therefore microalgae monocultures and mixed consortia could be described by an average value of $EC_{50,NH3}$ = 75 mg NH_3 L^{-1}. On the contrary, cyanobacteria growing in monocultures and mixed cultures were characterized by statistically different values of the inhibition parameter. In this case, an average value of $EC_{50,NH3}$ = 14 mg NH_3 L^{-1} was estimated for monocultures, which is significantly different from the $EC_{50,NH3}$ of 26 mg NH_3 L^{-1} obtained for mixed cultures (*p-value* = 0.029).

3.3. <u>Free ammonia inhibition scenarios in microalgae-based wastewater treatment</u>

The utilisation of parameter estimates for the obtained FA inhibition model can be particularly useful to evaluate the extent of the inhibition due to FA in several

common operational conditions of the phototrophs-bacteria cultivation processes. For example, rising TAN concentrations can result from limited removal rates during start-up periods or due to adverse atmospheric conditions. Similarly, the pH value can rise during the day, as a result of the photosynthetic activity. As an example, as explained in paragraph 2.5, the photosynthesis inhibition model was run using the time-series describing the daily evolution of FA during typical days in each scenario (i.e. by varying the season, the average pH and total TAN). To predict the FA response, eq. 9 was used with the estimated values of inhibition parameters (i.e., $EC_{50,NH3}$ = 88.4 mg NH_3 L^{-1} for microalgae-bacteria and $EC_{50,NH3}$ = 26.2 mg NH_3 L^{-1} for cyanobacteria-bacteria). The evolution of the inhibition function (f_{NH3}) under the identified environmental/operational conditions is depicted in Figure 4 for microalgae and cyanobacteria. Although the value of the microalgae-bacteria inhibition parameter is high, which means a high resistance to FA, severe inhibition levels can be reached under the worst conditions. In particular, the values of f_{NH3} during autumn indicate a photosynthesis inhibition of 30%, while the inhibition can reach values higher than 40%, during summer times. Temperature variations seem to have a lower influence on FA production, compared to the other parameters. When comparing summer and autumn, maximum f_{NH3} variations fall within 30% due to temperature variations, while larger effects are associated to the variation of other parameters (TAN and pH). At low and average pH, f_{NH3} is close to one, regardless of the TAN concentration or the seasonal condition imposed. A drastic drop in photosynthetic sOPRs occurs with higher pH values. Similarly, in the cyanobacterial mixed culture, the

inhibition function can result in a limited photosynthetic oxygen evolution during the day, due to the high pH values and temperatures. f_{NH3} can reach very low values (up to 75% inhibition), thus depicting severe inhibition, even if the considered TAN concentrations are seven times lower than those expected in HRAP scenarios. This clearly indicates the high influence of pH on FA generation, confirming that pH should be strictly controlled in wastewater treatment PBRs, to prevent reductions in the photosynthetic oxygenation by phototrophs.

For the microalgae-bacteria consortium case study, the trends for f_{TOT} and for the functions expressing the dependence of photosynthesis on FA and environmental conditions were also constructed. Switch functions are shown in Figure 5, for a TAN concentration of 60 mg N-TAN L^{-1} and for different seasons and pH conditions. Among the studied variables, temperature is the one most directly affecting photosynthetic sOPR: the value assumed by the f_T switch function is always the lowest (excluding the irradiance switch function, which is obviously zero during the night). This is particularly evident during autumn (Figure 5B and Figure 5D), when temperature is lower than the optimum. During summer, temperature approaches the optimal value, resulting in f_T close to one for almost all the daytime. Although summer temperatures are close to optimal values resulting in higher f_T values, the increase in temperature also favours the FA formation, what inhibits photosynthesis (Figure 5 A and Figure 5B). The combined effects of temperature and pH are evident when the pH is 9 (Figure 5C and Figure 5D): f_{TOT} reaches approximately 0.6-0.65 during summer and is reduced to approximately 0.5 during autumn. Regarding f_{NH3}, it has comparable

or lower values than the f_T during summer, indicating that under these conditions the inhibition due to FA is the most relevant limitation occurring in the reactor. It is also important to notice that the pH value can be responsible for a reduction of the photosynthetic activity in itself. This reduction is negligible at pH 7, but at a pH of 9 causes a reduction of approximately 15% of the sOPR.

CONCLUSIONS

Microalgae and cyanobacteria were differently inhibited by FA, with microalgae showing higher resistance than cyanobacteria. The simulation of different weather/operational conditions showed that FA can drastically impact photo-oxygenation processes in algae-bacteria wastewater treatment systems. The results suggest that considering FA inhibition in existing mathematical models describing microalgae/cyanobacteria-based wastewater treatment processes could lead to more reliable predictions and to a more rational design of treatment units. In addition, the proposed procedure can be used to generate a dataset of EC_{50} values and theoretical dose-response curves, for different chemicals known to be inhibitory for the algal-bacterial biomass (e.g. herbicides/pesticides or organic compounds).

Acknowledgements: SR and EF would like to thank Fondazione Cariplo (Project “Il Polo delle Microalghe - The Microalgae Hub”) for funding the experimentation, Prof. R.Casagrandi and the EnvLab (Politecnico di Milano) for hosting part of the experimentation, Prof. V.Mezzanotte, Dr. F.Marazzi, Dr. M.Mantovani (Università degli Studi di Milano - Bicocca) and Dr. M.Bellucci (Politecnico di Milano) for helpful discussions and for technical help in laboratory, Dr.A.Teli

(IDEA Bioprocess Technology s.r.l.) for realizing the photo-respirometer and for technical assistance. ER and RDM would like to thank the Spanish Ministries of Education, Culture and Sport, and Economy and Competitiveness for their research grants (FPU18/04941 and FJCI-2016-30997), respectively.

REFERENCES

1. Abeliovich, A., & Azov, Y. (1976). Toxicity of ammonia to algae in sewage oxidation ponds. *Applied and Environmental Microbiology*, *31*(6), 801–806.
2. Angelidaki, I., Ellegaard, L., & Ahring, B. K. (1991). A Mathematical Model for Dynamic Simulation of Anaerobic Digestion of Complex Substrates: Focusing on Ammonia Inhibition. *Biotechnology and Bioengineering*, *42*, 159–166.
3. Anthonisen, A. C., Loehr, R. C., S, P. T. B., & Srinath, E. G. (2012). Inhibition of nitrification by ammonia and nitrous acid. *Water Pollution Control Federation*, *48*(5), 835–852.
4. APHA (2017) Standard Methods for the Examination of Wastewater, 23rd edition. America Public Health Association, Washington, DC, USA.
5. ASCE. (1993). *Measurement of Oxygen Transfer in Clean Water*.
6. ASCE. (1996). *Standard Guidelines for In-Process Oxygen Transfer Testing*.
7. Azov, Y., & Goldman, J. C. (1982). Free ammonia inhibition of algal photosynthesis in intensive cultures. *Applied and Environmental Microbiology*, *43*(4), 735–9.
8. Belkin, S., & Boussiba, S. (1991). High internal pH conveys ammonia resistance in Spirulina platensis. *Bioresource technology*, *38*(2-3), 167-169.
9. Benson, B. B., & Krause, D. (1980). The concentration and isotopic fractionation of gases dissolved in freshwater in equilibrium with the atmosphere. 1. Oxygen. *Limnology and Oceanography*, *25*(4), 662–671.
10. Bernard, O., & Rémond, B. (2012). Validation of a simple model accounting for light and temperature effect on microalgal growth. Bioresource Technology, 123, 520–527. https://doi.org/10.1016/j.biortech.2012.07.022
11. Beyl, T., Louw, T. M., & Pott, R. W. (2019). Cyanobacterial growth in minimally amended anaerobic digestion effluent and flue-gas. *Microorganisms*, *7*(10), 428.
12. Campos, J. L., Valenzuela-Heredia, D., Pedrouso, A., Val del Río, A., Belmonte, M., & A, M.-C. (2016). Greenhouse Gases Emissions from Wastewater Treatment Plants : Minimization, Treatment, and Prevention. *Journal of Chemistry*.
13. Choi, O., Das, A., Yu, C. P., & Hu, Z. (2010). Nitrifying bacterial growth inhibition in the presence of algae and cyanobacteria. *Biotechnology and bioengineering*, *107*(6), 1004-1011.
14. Collos, Y., & Harrison, P. J. (2014). Acclimation and toxicity of high ammonium concentrations to unicellular algae. *Marine Pollution Bulletin*, *80*, 8–23. https://doi.org/10.1016/j.marpolbul.2014.01.006
15. Dai, G., Deblois, C. P., Liu, S., Juneau, P., & Qiu, B. (2008). Differential sensitivity of five cyanobacterial strains to ammonium toxicity and its inhibitory mechanism on the photosynthesis of rice-field cyanobacterium Ge–Xian–Mi (Nostoc). *Aquatic toxicology*, *89*(2), 113-121.
16. Drath, M., Kloft, N., Batschauer, A., Marin, K., Novak, J., & Forchhammer, K. (2008). Ammonia triggers photodamage of photosystem II in the cyanobacterium Synechocystis sp. strain PCC 6803. *Plant physiology*, *147*(1), 206-215.
17. Giannuzzi, L. (2019). Cyanobacteria Growth Kinetics. In Y. K. Wong (Ed.), *Algae* (pp. 1–17). IntechOpen. https://doi.org/10.5772/intechopen.81545
18. Goto, M., Nagao, N., Yusoff, F. M., Kamarudin, M. S., Katayama, T., Kurosawa, N., ... & Toda, T. (2018). High ammonia tolerance on growth rate of marine microalga Chlorella vulgaris. *Journal of Environmental Biology*, *39*(5), 843-848.
19. Gutierrez, J., Kwan, T. A., Zimmerman, J. B., & Peccia, J. (2016). Ammonia inhibition in oleaginous microalgae. *Algal Research*, *19*, 123–127. https://doi.org/10.1016/j.algal.2016.07.016
20. Han, K., & Levenspiel, O. (1987). Extended Monod kinetics for Substrate, Product, and Cell Inhibition. *Biotechnology and Bioengineering*, *32*, 430–437. https://doi.org/10.1093/nq/s5-VIII.188.83

21. Hernández, D., Riaño, B., Coca, M., & García-González, M. C. (2013). Treatment of agro-industrial wastewater using microalgae–bacteria consortium combined with anaerobic digestion of the produced biomass. *Bioresource technology*, *135*, 598-603.
22. Hurvich, C. M., & Tsai, C. L. (1991). Bias of the corrected AIC criterion for underfitted regression and time series models. *Biometrika*, *78*(3), 499-509.
23. Ippoliti, D., Gómez, C., del Mar Morales-Amaral, M., Pistocchi, R., Fernández-Sevilla, J. M., & Acién, F. G. (2016). Modeling of photosynthesis and respiration rate for Isochrysis galbana (T-Iso) and its influence on the production of this strain. *Bioresource Technology*, *203*, 71–79. https://doi.org/10.1016/j.biortech.2015.12.050
24. Källqvist, T., & Svenson, A. (2003). Assessment of ammonia toxicity in tests with the microalga, Nephroselmis pyriformis, Chlorophyta. *Water research*, *37*(3), 477-484.
25. Li, X., Li, W., Zhai, J., Wei, H., & Wang, Q. (2019). Effect of ammonium nitrogen on microalgal growth, biochemical composition and photosynthetic performance in mixotrophic cultivation. *Bioresource technology*, *273*, 368-376.
26. Mantovani, M., Marazzi, F., Fornaroli, R., Bellucci, M., Ficara, E., & Mezzanotte, V. (2019). Outdoor pilot-scale raceway as a microalgae-bacteria sidestream treatment in a WWTP. *Science of the Total Environment* (in press), 135583. https://doi.org/10.1016/j.scitotenv.2019.135583
27. Marazzi, F., Bellucci, M., Rossi, S., Fornaroli, R., Ficara, E., & Mezzanotte, V. (2019). Outdoor pilot trial integrating a sidestream microalgae process for the treatment of centrate under non optimal climate conditions. *Algal Research*, *39*, 101430. https://doi.org/10.1016/j.algal.2019.101430
28. Markou, G., Vandamme, D., & Muylaert, K. (2014). Ammonia inhibition on Arthrospira platensis in relation to the initial biomass density and pH. *Bioresource Technology*, *166*, 259–265. https://doi.org/10.1016/j.biortech.2014.05.040
29. Markou, G., & Muylaert, K. (2016). Effect of light intensity on the degree of ammonia toxicity on PSII activity of Arthrospira platensis and Chlorella vulgaris. *Bioresource technology*, *216*, 453-461.
30. Markou, G., Depraetere, O., & Muylaert, K. (2016). Effect of ammonia on the photosynthetic activity of Arthrospira and Chlorella: A study on chlorophyll fluorescence and electron transport. *Algal Research*, *16*, 449–457. https://doi.org/10.1016/j.algal.2016.03.039
31. Moreno-garcia, L., Adjallé, K., Barnabé, S., & Raghavan, G. S. V. (2017). Microalgae biomass production for a biore fi nery system: Recent advances and the way towards sustainability. *Renewable and Sustainable Energy Reviews*, *76*(May 2016), 493–506. https://doi.org/10.1016/j.rser.2017.03.024
32. Muñoz, R., & Guieysse, B. (2006). Algal – bacterial processes for the treatment of hazardous contaminants : A review. *Water Research*, *40*, 2799–2815. https://doi.org/10.1016/j.watres.2006.06.011
33. Najm, Y., Jeong, S., & Leiknes, T. (2017). Nutrient utilization and oxygen production by Chlorella vulgaris in a hybrid membrane bioreactor and algal membrane photobioreactor system. *Bioresource technology*, *237*, 64-71.
34. Plappally, A. K., & Lienhard, J. H. V. (2012). Energy requirements for water production, treatment, end use, reclamation, and disposal. *Renewable and Sustainable Energy Reviews*, *16*(7), 4818–4848. https://doi.org/10.1016/j.rser.2012.05.022
35. Prinz, H. (2010). Hill coefficients , dose – response curves and allosteric mechanisms. *Journal of Chemical Biology*, *3*, 37–44. https://doi.org/10.1007/s12154-009-0029-3
36. Rada-Ariza, A. (2018). Photo-Activated Sludge: A Novel Algal-Bacterial Biotreatment for Nitrogen Removal from Wastewater. IHE-Delft Institute for Water Education. https://doi.org/10.1201/9780429058257
37. Rossi, S., Bellucci, M., Marazzi, F., Mezzanotte, V., & Ficara, E. (2018). Activity assessment of microalgal-bacterial consortia based on respirometric tests. *Water Science and Technology*, *78*(1), 207–215. https://doi.org/10.2166/wst.2018.078
38. Rossi, S., Sforza, E., Pastore, M., Bellucci, M., Casagli, F., Marazzi, F., Ficara, E. (2020a) Photo-respirometry to shed light on microalgae-bacteria consortia—a review.

Reviews in Environmental Science and Bio/Technology (in press), 1-30. https://doi.org/10.1007/s11157-020-09524-2

39. Rossi, S., Casagli, F., Mantovani, M., Mezzanotte, V., Ficara, E. (2020b) Selection of photosynthesis and respiration models to assess the effect of environmental conditions on mixed microalgae consortia grown on wastewater. *Bioresource technology* (in press), 122995. https://doi.org/10.1016/j.biortech.2020.122995
40. Rueda, E., García-galán, M. J., Díez-montero, R., Vila, J., Grifoll, M., & García, J. (2020). Polyhydroxybutyrate and glycogen production in photobioreactors inoculated with wastewater borne cyanobacteria monocultures. *Bioresource Technology*, *295*(August 2019), 122233. https://doi.org/10.1016/j.biortech.2019.122233
41. Rueda, E., García-Galán, M.J., Ortiz, A., Uggetti, E., Carretero, J., García, J., Díez-Montero, R. (2020) Bioremediation of agricultural runoff and biopolymers production from Cyanobacteria cultured in demonstrative full-scale photobioreactors. *Process Safety and Environmental Protection* (submitted)
42. Sander, R. (2015). Compilation of Henry's law constants (version 4.0) for water as solvent. *Atmospheric Chemistry and Physics*, *15*, 4399–4981. https://doi.org/10.5194/acp-15-4399-2015
43. Segura, C., Vergara, C., Seeger, M., Donoso-Bravo, A., & Jeison, D. (2017). When constants are no longer constant: The case of inhibition in bioprocesses. *Biochemical Engineering Journal*, *123*, 24-28.
44. Shoener, B. D., Schramm, S. M., Béline, F., Bernard, O., Martínez, C., Plósz, B. G., ... & Guest, J. S. (2019). Microalgae and cyanobacteria modeling in water resource recovery facilities: A critical review. *Water research X*, *2*, 100024.
45. Tam, N. F. Y., & Wong, Y. S. (1996). Effect of ammonia concentrations on growth of Chlorella vulgaris and nitrogen removal from media. *Bioresource Technology*, *57*(1), 45–50. https://doi.org/10.1016/0960-8524(96)00045-4
46. Tan, X. B., Zhang, Y. L., Yang, L. B., Chu, H. Q., & Guo, J. (2016). Outdoor cultures of Chlorella pyrenoidosa in the effluent of anaerobically digested activated sludge: the effects of pH and free ammonia. *Bioresource technology*, *200*, 606-615.
47. Tang, T., Fadaei, H., & Hu, Z. (2014). Rapid evaluation of algal and cyanobacterial activities through specific oxygen production rate measurement. *Ecological engineering*, *73*, 439-445.
48. Wang, J., Zhou, W., Chen, H., Zhan, J., He, C., & Wang, Q. (2019). Ammonium Nitrogen Tolerant Chlorella Strain Screening and Its Damaging Effects on Photosynthesis. *Frontiers in Microbiology*, *9*, 3250. https://doi.org/10.3389/fmicb.2018.03250
49. Van Loosdrecht, M. C., Nielsen, P. H., Lopez-Vazquez, C. M., & Brdjanovic, D. (2016). *Experimental methods in wastewater treatment*. IWA publishing.

Figure captions

Figure 1. Scheme of the experimental setup for photo-respirometric test. Legend: 1 = Mixing and signal communication unit, 2 = Glass bottles, 3 = DO, temperature and pH probes, 4 = Acid/base dosage pumps, 5 = Air/gas pumps, 6 = Normally closed electro-valves, 7 = Gas cylinder (CO_2/O_2/N_2), 8 = Acid/base solutions, 9 = Industrial grade PC, 10 = light source.

Figure 2. Effects of free ammonia inhibition on microalgae and cyanobacteria: reduction of f_{NH3}, non-competitive inhibition model fit and estimated model parameters (A: Microalgae, B: Cyanobacteria). Samples abbreviations: M_1 = *Chlorella vulgaris sp.*, M_2 = *Scenedesmus quadricauda sp.*, M_3 = *Chlorella sorokiniana sp.*, M_4 = *Scenedesmus obliquus sp.*, MB = Sample from the HRAP; C1 = *Synechocystis sp.*, C2 = *Synechococcus sp.*, C3 = *Leptolyngbya sp.*, CB_1 = Sample from the semi-closed PBR_1, CB_2 = Sample from the semi-closed PBR_2, CB_3 = Sample from the semi-closed PBR_3. Shaded areas and error bars represent 95% confidence intervals.

Figure 3. Typical daily variations of water temperature and irradiance for different seasons (A = water temperature in the HRAP, B = water temperature in semi-closed PBRs, C = irradiance data for the HRAP, dataset: January 2017 - November 2019).

Figure 4*.* Simulated evolution of the inhibition function (f_{NH3}) under typical daily variations for different seasons, pH values and TAN concentrations. Inhibition functions are calculated considering microalgae (A - D) and cyanobacteria (E - H) as dominant species in mixed phototrophs-bacteria consortia.

Figure 5*.* Simulated evolution of switch functions in the HRAP at 60 mg N-TAN L^{-1} for different seasons and pH values (A = summer, low pH, B = autumn, low pH, C = summer, high pH, D = autumn, high pH).

Table captions

Table 1. Free ammonia inhibition tests performed and conditions applied. Temperature and irradiance data are reported as mean ± standard deviation.

Table 2. Selection criteria and estimated parameters for selected free ammonia inhibition models. 95% confidence intervals on estimated parameters are reported in square brackets. Averaged data are reported as mean ± standard deviation.

Figure 6.

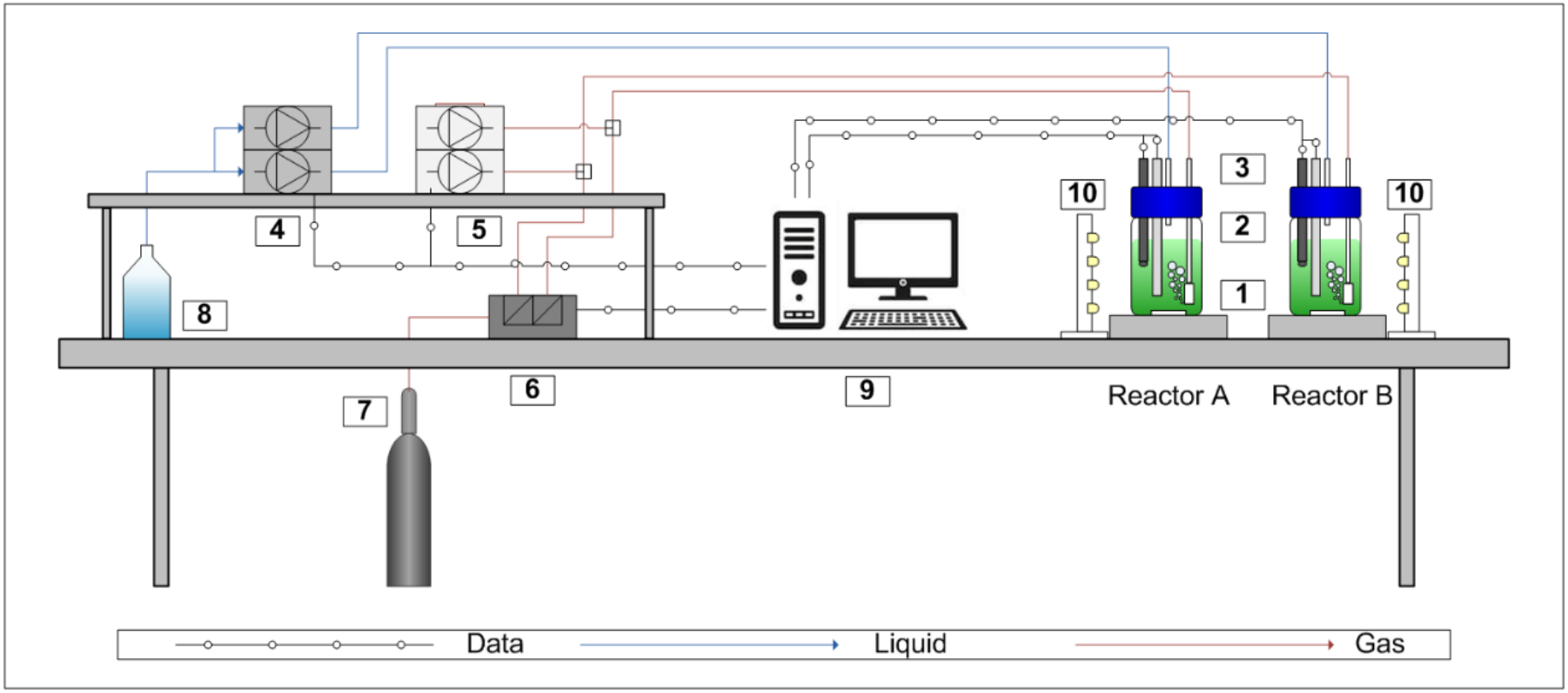

Figure 7.

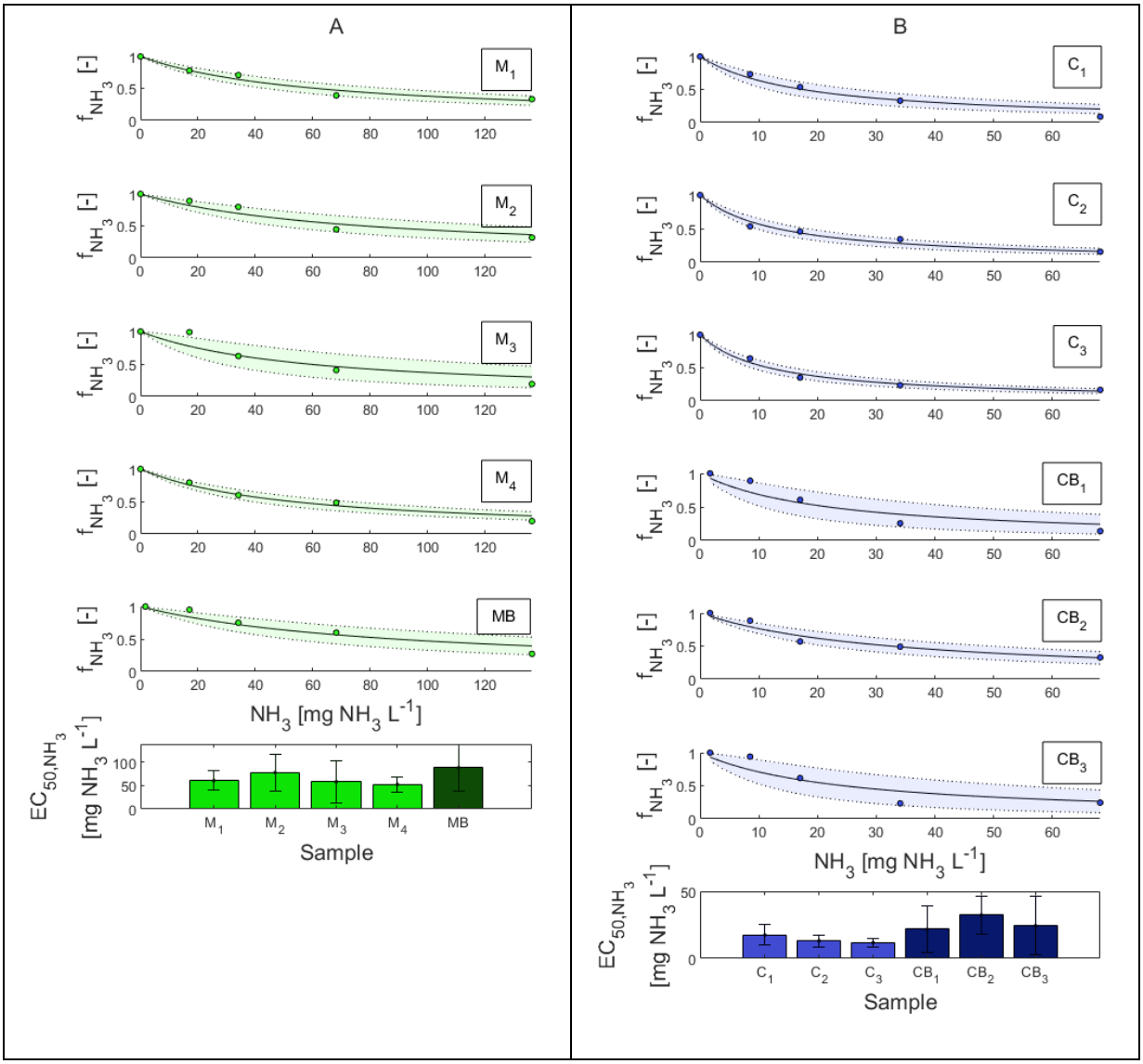
A
B
M1
M2
M3
M4
MB
C1
C2
C3
CB1
CB2
CB3
fNH3 [-]
NH3 [mg NH3 L-1]
EC50,NH3 [mg NH3 L-1]
Sample

Figure 3

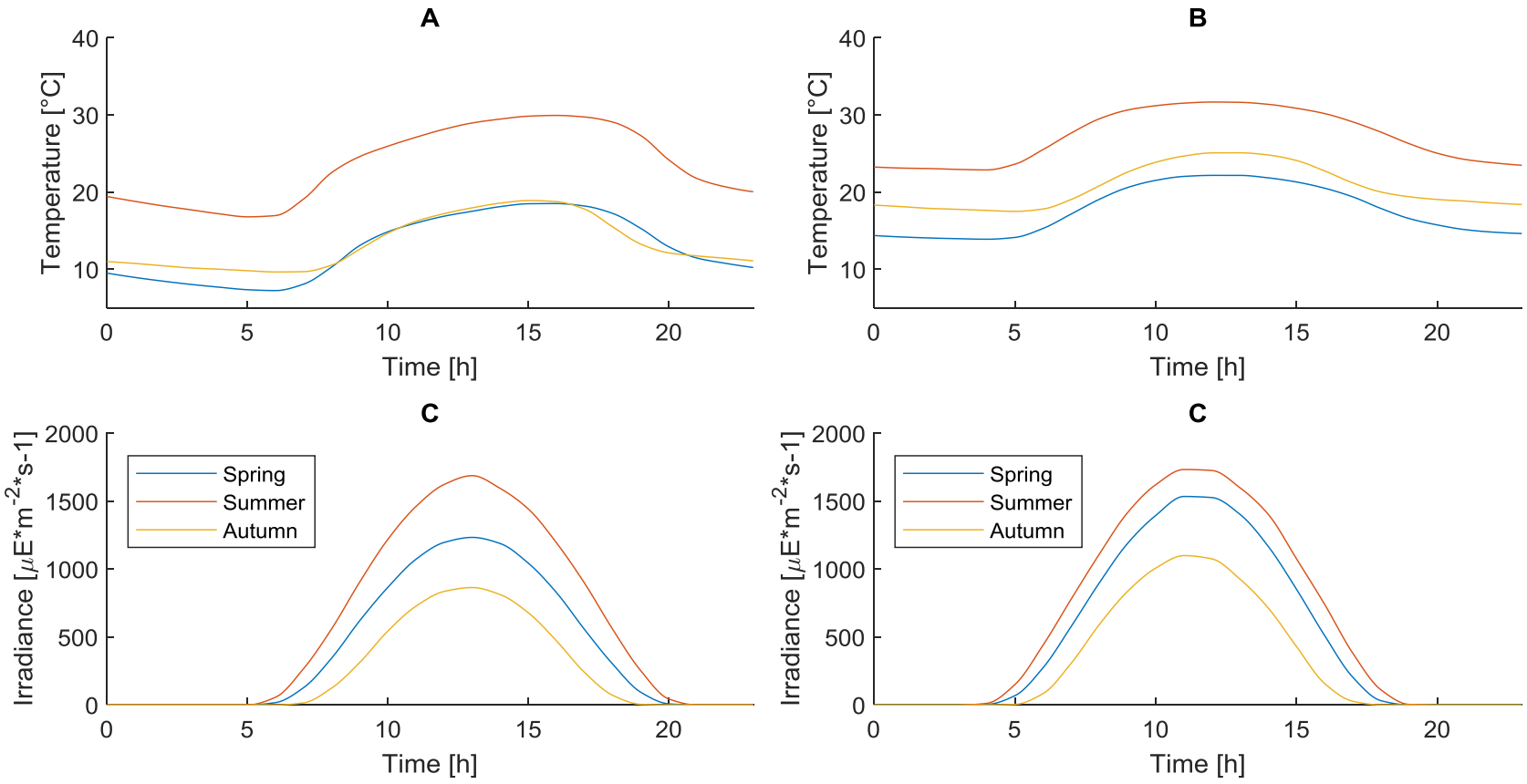
A
B
C
C
Temperature [°C]
Irradiance [μE*m-2*s-1]
Time [h]
Spring
Summer
Autumn
0
5
10
15
20
10
20
30
40
500
1000
1500
2000

Figure 4.

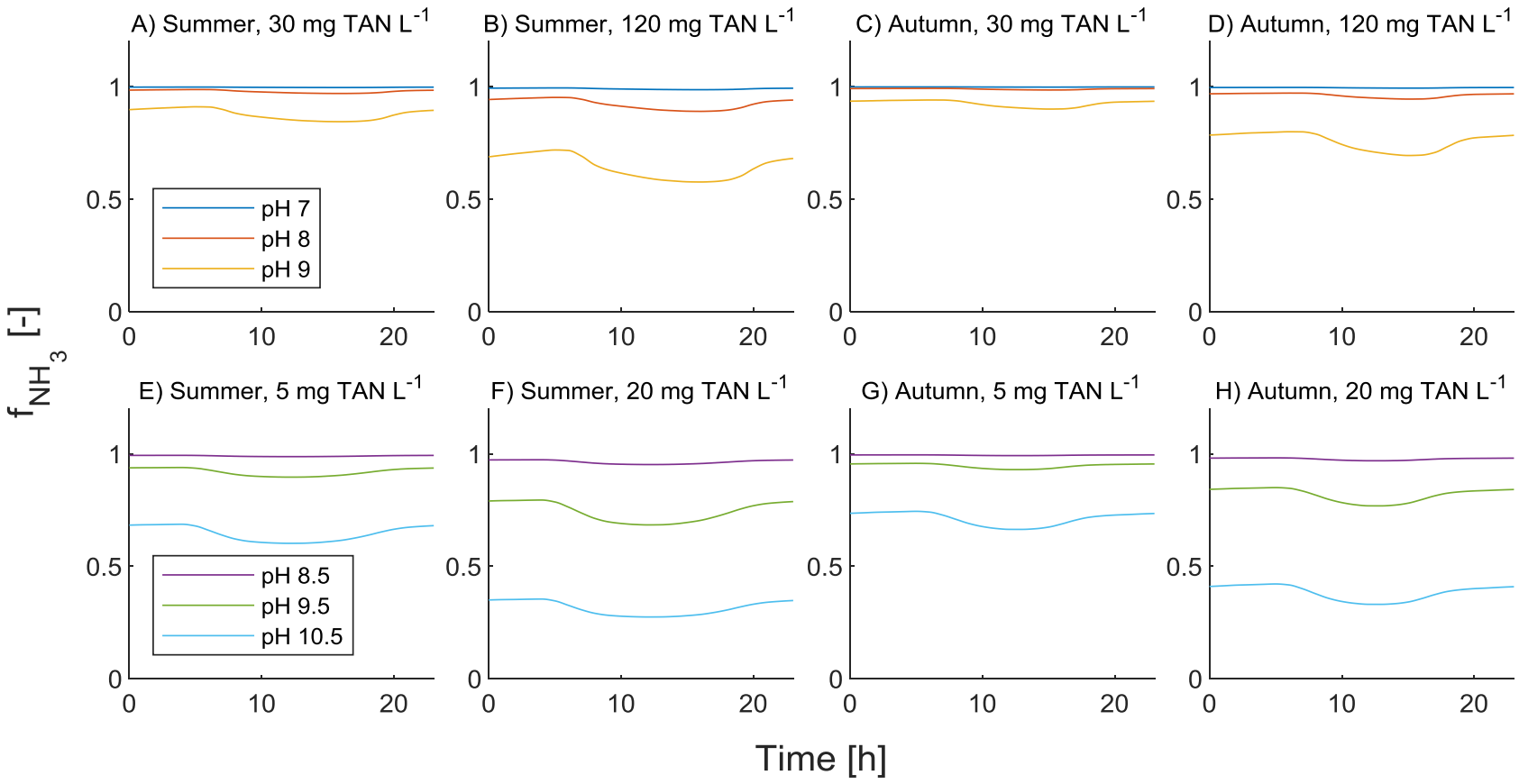
A) Summer, 30 mg TAN L-1
B) Summer, 120 mg TAN L-1
C) Autumn, 30 mg TAN L-1
D) Autumn, 120 mg TAN L-1
E) Summer, 5 mg TAN L-1
F) Summer, 20 mg TAN L-1
G) Autumn, 5 mg TAN L-1
H) Autumn, 20 mg TAN L-1
pH 7
pH 8
pH 9
pH 8.5
pH 9.5
pH 10.5
f NH3 [-]
Time [h]

Figure 5.

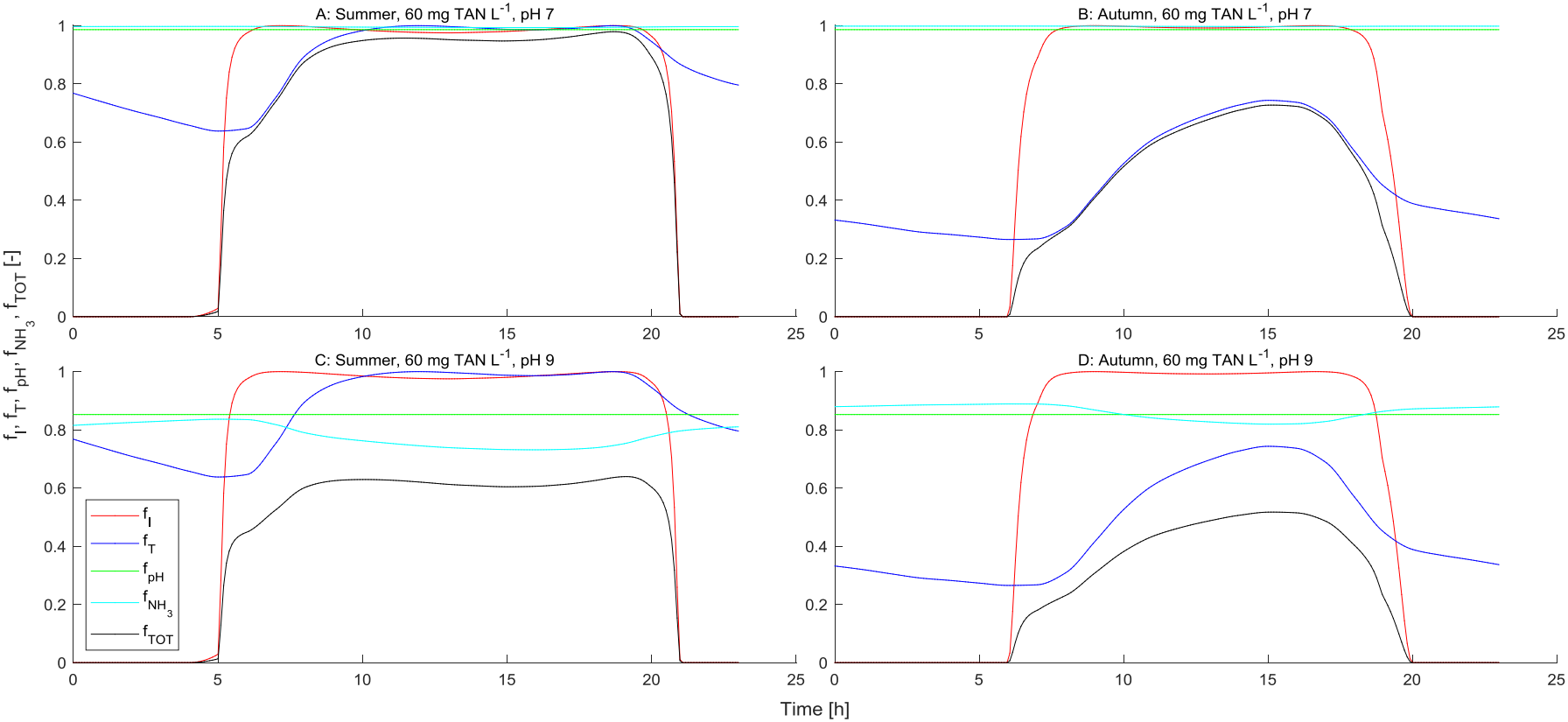
A: Summer, 60 mg TAN L-1, pH 7
B: Autumn, 60 mg TAN L-1, pH 7
C: Summer, 60 mg TAN L-1, pH 9
D: Autumn, 60 mg TAN L-1, pH 9
fI, fT, fpH, fNH3, fTOT [-]
Time [h]
fI
fT
fpH
fNH3
fTOT

Table 3.

Test ID	Cultivation system (volume)	Type of culture and dominant phototrophs	Species	Growth substrate (N-source)	Free ammonia concentration	Temperature	Irradiance
-	-	-	-	-	mg NH_3 L^{-1}	°C	µE m^{-2} s^{-1}
MB	HRAP (1.2 m^3)	Phototrophs-bacteria	*Chlorella/Scenedesmus sp.*	Anaerobic digestate (NH_4)	17, 34, 68, 134	20.3 ± 0.2	108 ± 16
CB_1	Semi-closed PBRs (11.7 m^3)	Phototrophs-bacteria	*Synechocystis sp.*, *Synechococcus sp.*	Agricultural runoff (NO_3)	8.5, 17, 34, 68	21.5 ± 0.3	116 ± 23
CB_2	Semi-closed PBRs (11.7 m^3)	Phototrophs-bacteria	*Synechocystis sp.*, *Synechococcus sp.*	Agricultural runoff (NO_3)	8.5, 17, 34, 68	21.6 ± 0.3	116 ± 23
CB_3	Semi-closed PBRs (11.7 m^3)	Phototrophs-bacteria	*Synechocystis sp.*, *Synechococcus sp.*	Agricultural runoff (NO_3)	8.5, 17, 34, 68	21.8 ± 0.4	116 ± 23
M_1	Lab-scale PBR (1 L)	Green algae monoculture	*Chlorella vulgaris*	MBBM (NO_3)	17, 34, 68, 134	19.6 ± 0.1	108 ± 16
M_2	Lab-scale PBR (1 L)	Green algae monoculture	*Scenedesmus quadricauda*	MBBM (NO_3)	17, 34, 68, 134	19.7 ± 0.1	108 ± 16
M_3	Lab-scale PBR (1 L)	Green algae monoculture	*Chlorella sorokiniana*	MBBM (NO_3)	17, 34, 68, 134	19.9 ± 0.1	108 ± 16
M_4	Lab-scale PBR (1 L)	Green algae monoculture	*Scenedesmus obliquus*	MBBM (NO_3)	17, 34, 68, 134	20 ± 0.0	108 ± 16
C_1	Lab-scale PBR (1 L)	Cyanobacteria monoculture	*Synechocystis sp.*	BG11 (NO_3)	8.5, 17, 34, 68	20.0 ± 0.4	116 ± 23
C_2	Lab-scale PBR (1 L)	Cyanobacteria monoculture	*Synechococcus sp.*	BG11 (NO_3)	8.5, 17, 34, 68	20.6 ± 0.3	116 ± 23
C_3	Lab-scale PBR (1 L)	Cyanobacteria monoculture	*Leptolyngbia sp.*	BG11 (NO_3)	8.5, 17, 34, 68	20.8 ± 0.3	116 ± 23

Table 4.

Test ID	Cyanobacteria					
	Model 1 (Non-competitive inhibition)			Model 2 (Sigmoidal logistic function)		
	cAIC	R_{ADJ}^2	Estimated parameters	cAIC	R_{ADJ}^2	Estimated parameters
C_1	-16.7	0.9478	$EC_{50,NH3}$ = 17.5 mg NH_3 L^{-1} [9.9, 25.0]	-17.8	0.9820	$EC_{50,NH3}$ = 18.5 mg NH_3 L^{-1} [14.7, 22.2], N = 1.43 [0.96, 1.89]
C_2	-19.7	0.9990	$EC_{50,NH3}$ = 13.1 mg NH_3 L^{-1} [8.8, 17.5]	-16.1	0.9993	$EC_{50,NH3}$ = 11.8 mg NH_3 L^{-1} [6.1, 17.5], N = 0.78 [0.34, 1.21]
C_3	-21.0	0.9982	$EC_{50,NH3}$ = 11.7 mg NH_3 L^{-1} [8.2, 15.2]	-15.3	0.9981	$EC_{50,NH3}$ = 12.3 mg NH_3 L^{-1} [7.9, 16.6], N = 1.15 [0.58, 1.71]
Avg	-	-	*$EC_{50,NH3}$ = 14.1 ± 3.0 mg NH_3 L^{-1}*	-	-	*$EC_{50,NH3}$ = 14.2 ± 3.7 mg NH_3 L^{-1}, N = 1.12 ± 0.32*
CB_1	-10.3	0.9972	$EC_{50,NH3}$ = 21.8 mg NH_3 L^{-1} [4.4, 39.2]	-17.6	0.9998	$EC_{50,NH3}$ = 21.4 mg NH_3 L^{-1} [17.8, 25.0], N = 2.01 [1.37, 2.67]
CB_2	-16.6	0.9983	$EC_{50,NH3}$ = 32.4 mg NH_3 L^{-1} [18.4, 46.5]	-10.4	0.9979	$EC_{50,NH3}$ = 31.6 mg NH_3 L^{-1} [15.3, 47.9], N = 1.12 [0.33, 1.91]
CB_3	-9.3	0.9832	$EC_{50,NH3}$ = 24.4 mg NH_3 L^{-1} [2.8, 46.1]	-7.4	0.9903	$EC_{50,NH3}$ = 22.7 mg NH_3 L^{-1} [11.8, 33.6], N = 1.92 [0.23, 3.61]
Avg	-	-	*$EC_{50,NH3}$ = 26.2 ± 5.5 mg NH_3 L^{-1}*	-	-	*$EC_{50,NH3}$ = 25.2 ± 5.6 mg NH_3 L^{-1}, N = 1.68 ± 0.49*
	Microalgae					
Test ID	**Model 1 (Non-competitive inhibition)**			**Model 2 (Sigmoidal logistic function)**		
	cAIC	**R_{ADJ}^2**	**Estimated parameters**	**cAIC**	**R_{ADJ}^2**	**Estimated Parameters**
M_1	-18.8	0.9996	$EC_{50,NH3}$ = 60.9 mg NH_3 L^{-1} [39.7, 82.1]	-12.4	0.9995	$EC_{50,NH3}$ = 60.3 mg NH_3 L^{-1} [34.5, 86.1], N = 1.08 [0.42, 1.75]
M_2	-15.1	0.9996	$EC_{50,NH3}$ = 77.7 mg NH_3 L^{-1} [37.7, 117.7]	-13.6	0.9998	$EC_{50,NH3}$ = 71.1 mg NH_3 L^{-1} [49.0, 93.1], N = 1.49 [0.73, 2.24]
M_3	-12.7	0.9960	$EC_{50,NH3}$ = 96.3 mg NH_3 L^{-1} [31.2, 161.3]	-9.5	0.9972	$EC_{50,NH3}$ = 54.2 mg NH_3 L^{-1} [34.2, 74.2], N = 1.80 [0.62, 2.97]
M_4	-19.6	0.9993	$EC_{50,NH3}$ = 52.6 mg NH_3 L^{-1} [26.1, 66.4]	-15.3	0.9994	$EC_{50,NH3}$ = 52.4 mg NH_3 L^{-1} [37.1, 67.7], N = 1.20 [0.68, 1.73]
MB	-14.2	0.9994	$EC_{50,NH3}$ = 88.4 mg NH_3 L^{-1} [37.9, 138.9]	-16.6	0.9999	$EC_{50,NH3}$ = 78.7 mg NH_3 L^{-1} [61.5, 95.9], N = 1.63 [1.01, 2.26]
Avg	-	-	*$EC_{50,NH3}$ = 75.2 ± 18.3 mg NH_3 L^{-1}*	-	-	*$EC_{50,NH3}$ = 63.3 ± 11.3 mg NH_3 L^{-1}, N = 1.44 ± 0.30*